Development 138, 4733-4741 (2011) doi:10.1242/dev.072496

The transcription factor BELLRINGER modulates phyllotaxis by regulating the expression of a pectin methylesterase in *Arabidopsis*

Alexis Peaucelle[1], Romain Louvet[2], Jorunn N. Johansen[1,*], Fabien Salsac[1], Halima Morin[1], Françoise Fournet[2], Katia Belcram[1], Françoise Gillet[2], Herman Höfte[1], Patrick Laufs[1], Grégory Mouille[1] and Jérôme Pelloux[2,†]

SUMMARY

Plant leaves and flowers are positioned along the stem in a regular pattern. This pattern, which is referred to as phyllotaxis, is generated through the precise emergence of lateral organs and is controlled by gradients of the plant hormone auxin. This pattern is actively maintained during stem growth through controlled cell proliferation and elongation. The formation of new organs is known to depend on changes in cell wall chemistry, in particular the demethylesterification of homogalacturonans, one of the main pectic components. Here we report a dual function for the homeodomain transcription factor BELLRINGER (BLR) in the establishment and maintenance of the phyllotactic pattern in *Arabidopsis*. BLR is required for the establishment of normal phyllotaxis through the exclusion of pectin methylesterase *PME5* expression from the meristem dome and for the maintenance of phyllotaxis through the activation of *PME5* in the elongating stem. These results provide new insights into the role of pectin demethylesterification in organ initiation and cell elongation and identify an important component of the regulation mechanism involved.

KEY WORDS: Cell wall, Pectins, Pectin methylesterase (PME), Shoot apical meristem, Phyllotaxis, *Arabidopsis*

INTRODUCTION

The multitude of shapes adopted by multicellular organisms are controlled by complex networks of regulatory genes. How these regulatory networks are translated into the local changes in tissue growth that underlie morphogenesis remains a central question in developmental biology.

Plants are useful models with which to study organogenesis as new organs are formed throughout their lives, in contrast to animals in which organogenesis is restricted to embryogenesis. The shoot apical meristem (SAM), which gives rise to all aerial organs of the plant, has a dual function: maintaining a pool of undifferentiated cells, and initiating new lateral organs according to a specific temporal and spatial pattern, known as phyllotaxis (Carraro et al., 2006). Beyond the meristem, the phyllotactic pattern is actively maintained during stem growth. This process requires the restriction of the CUC2 transcription factor to the boundary domain, which involves miR164 (Peaucelle et al., 2007; Sieber et al., 2007).

The homeodomain transcription factors belonging to the KNOX and BEL groups play key roles in both meristem maintenance and organ patterning (Carraro et al., 2006; Smith et al., 2004). The KNOX and BEL transcription factors, which can form various heterodimers, regulate the expression of different sets of downstream effectors. BELLRINGER (BLR; also known as PENNYWISE, REPLUMLESS or VAAMANA) (Byrne et al., 2003; Kanrar et al., 2006; Roeder et al., 2003; Smith and Hake, 2003) is one of the members of the BEL group expressed in the meristem. The *blr* mutant was first described for its abnormal phyllotaxis, but also presents other developmental defects (Byrne et al., 2003; Kanrar et al., 2006; Kanrar et al., 2008; Roeder et al., 2003; Smith and Hake, 2003). *BLR* also shows complex genetic interactions with other BEL and KNOX genes (Smith and Hake, 2003; Smith et al., 2004; Ragni et al., 2008; Rutjens et al., 2009; Ung et al., 2011) and directly represses the flower organ identity gene *AGAMOUS* during flower development (Bao et al., 2004).

The initiation of new lateral organs depends on the local accumulation of the phytohormone auxin (Bayer et al., 2009; Reinhardt et al., 2000; Reinhardt et al., 2003). The auxin distribution within the meristem is highly dynamic and is the result of passive diffusion and active cell-to-cell transport involving the efflux carrier PIN1 and various influx carriers (Bainbridge et al., 2008). In several mathematical models, auxin patterning is autoregulated through feedback loops linking auxin flux or auxin accumulation (Jonsson et al., 2006; Smith et al., 2006; Stoma et al., 2008) to the polar intracellular localisation of PIN1. At the position of the auxin maximum a new organ primordium is initiated. The developing organ is thought to act as an auxin sink, which leads to the redistribution of the auxin and to the emergence of a new maximum at the position of the future primordium. In parallel to auxin patterning, the chemical modification of a cell wall component – the demethylesterification of the pectic polysaccharide homogalacturonan (HG) – also plays a key role in triggering primordia formation (Peaucelle et al., 2008).

Pectins, which represent ~35% of the dry weight in dicotyledonous species, are complex polysaccharides rich in galacturonic acid (Caffall and Mohnen, 2009; Mohnen, 2008). HG, one of the main pectic constituents, is a linear homopolymer of α-(1-4)-linked D-galacturonic acids, which can be methylesterified at

[1]Institut Jean-Pierre Bourgin, UMR1318 INRA-AgroParisTech, Bâtiment 2, INRA Centre de Versailles-Grignon, Route de St Cyr (RD 10), 78026 Versailles Cedex, France. [2]EA3900-BIOPI Biologie des Plantes et Innovation, Université de Picardie, 33 Rue St Leu, 80039 Amiens, France.

*Present address: Institute for Cancer Research, Department of Immunology, Rikshospitalet-Radiumhospitalet, Medical Centre, Montebello 0310 Oslo, Norway
†Author for correspondence (jerome.pelloux@u-picardie.fr)

Accepted 30 August 2011

the C-6 carboxyl residue. HG is synthesized from nucleotide sugars by a variety of glycosyl transferases (Lerouxel et al., 2006) in the Golgi apparatus and secreted in a highly methylesterified form into the cell wall (Sterling et al., 2001). Subsequently, its structure can be altered by the activity of cell wall-based enzymes. For example, the degree of methylesterification can be modified by pectin methylesterases (PMEs, EC 3.1.1.11), the activity of which is in turn regulated by proteinaceous PME inhibitors (PMEIs) (Pelloux et al., 2007). Both PMEs and PMEIs are members of large gene families (66 and 69 members, respectively, in *Arabidopsis*).

The similarity of the defects in phyllotaxis observed in the *Arabidopsis blr* mutant and following ectopic pectin demethylesterification prompted us to investigate the link between these two factors. Here, we report that ectopic primordia formation in the floral meristem of *blr* is the result of meristem-specific changes in the PME-mediated methylesterification status of HG as a result of the ectopic expression of one member of the PME family, PME5. The ectopic primordia formation was reversed in the *blr*/*pme5* double mutant, confirming unequivocally the role of PME5 in this process. Furthermore, we show that, in the *blr* mutant, the downregulation of *PME5* expression in the internode leads to a defect in internode elongation that is associated with reduced cell expansion. In addition to identifying part of the regulatory network that controls the methylesterification status of HG in the stem, our results further confirm the crucial role of the demethylesterification of HG in the regulation of cell elongation.

MATERIALS AND METHODS

Plant material and growth conditions

The *blr-6* mutant was identified, based on its phenotype, in the Versailles T-DNA insertion collection (WS ecotype). Tests for allelism were carried out by crossing plants homozygous for *pny-42016* (Smith and Hake, 2003) with plants homozygous for *blr-6*. F1 plants displayed the *blr* mutant phenotype, showing that *blr-6* and *pny-420169* are allelic. The right and left flanking sequences of the T-DNA insertion site were amplified by PCR in the *blr-6* mutant using the T-DNA-specific primer Tag5 (5′-CTACAAATTGCCTTTTCTTATCGAC-3′) and the gene-specific primers pny-04 (Smith and Hake, 2003) and Tag3 (5′-CTGATACCAGACGTTGCCCGCATAA-3′) and pny-3, respectively (Smith and Hake, 2003). Sequencing of the PCR products showed that the T-DNA was inserted in the first intron, at position 1262 to 1271 relative to the initiation codon.

pme5-1 and *pme5-2* mutants were isolated from the Versailles T-DNA insertion collection (WS ecotype). The left flanking sequence of the T-DNA insertion site was amplified by PCR using Tag5 and the *At5g47500* gene-specific primers 5′-CTCCGACCGTTTCCTTTCTCA-3′ and 5′-GCATCACAATCAAGATTGCTCC-3′ for lines FLAG_175B12 and FLAG_232E12, respectively. PCR products were sequenced and the site of insertion confirmed.

Plant growth in controlled chambers under short-day or long-day conditions was as described previously (Deveaux et al., 2003).

Electron microscopy and phyllotactic pattern measurement

Scanning electron microscopy, confocal microscopy, epidermal cell length measurement and phyllotactic pattern measurement have been described previously (Peaucelle et al., 2008). For each experiment, phyllotaxis measurements were performed on a minimum of five plants and meristematic phyllotaxis measurements on a minimum of ten plants. Cell lengths were measured on at least three internodes from at least five different plants. The Kolmogorov-Smirnov (K-S) test was performed.

Fourier transform infrared (FTIR) microscopy

Ten 12 μm slices from ten meristems of ten different wild-type and *blr-6* plants were obtained by Vibratome sectioning of dissected dried inflorescences embedded in 5% low-melting-point agarose. For each meristem slice, ten FTIR spectra were collected from the central zone of the meristem. Spectra were baselined and area-normalised as described (Mouille et al., 2003). Statistical analyses were performed as described (Mouille et al., 2003).

PME activity measurements

PME activity was assayed using the alcohol oxidase-coupled assay on cell wall-enriched total protein extracts as described (Klavons and Bennet, 1986). Protein concentration in extracts was measured according to Bradford (Bradford, 1976) using a protein assay kit (Bio-Rad, Marnes-la-Coquette, France). Data are the mean of four to six independent replicates. Data were statistically analysed by the Mann-Whitney test (Statisca, Statsoft, Maison-Alfort, France).

Real-time quantitative PCR (RT-qPCR)

Following RNA extraction from floral buds and cDNA synthesis, *At5g09760*, *At3g19730*, *At5g47500*, *At4g33220* and *At3g49220* transcripts were quantified by RT-qPCR using the following specific primers (5′ to 3′): *At5g09760*, GGGAGGCCATGGAAAGATTA and AGCAGACA-TCGAAGCCCACTC; *At3g19730*, ATAAGCTAGGAGCAGTGACG and ATTCAGAGCCGTCGATAAAGG; *At5g47500*, ATGGCCGCTCCATGT-ATAAAG/CTCTCGTCGCTGCTGCTCCT; *At4g33220*, CCGGAAAGA-TGTCAACCAAC and AAGGCAGCCAAAGATTTCCT; *At3g49220*, CATGCGTCTAGGGTTCTTGC and AATCCGGCCAAGAACGAAAC; *UBQ5* (*At3g62250*) was used as reference (GACGCTTCATCTCGTCC and CCACAGGTTGCGTTAG). Reactions were performed in a Roche LightCycler using the FastStart DNA MasterPLUS SYBR Green I Kit (Roche). Data are the mean of four to six replicates. These data were exported into RelQuant (Roche), which provides efficiency-corrected normalised quantification results. For each candidate gene, the expression in *blr-6* is given relative to that in the wild type, which was set at 1.

β-glucuronidase (GUS) staining and imaging

A 1 kb region of the *At5g47500* promoter was amplified using Phusion Hot Start F-Taq Polymerase (Finnzyme, Saint Quentin en Yvelines, France). The PCR product was cloned into the pGEM-T Easy vector (Promega, Charbonnières-les-Bains, France), sequenced and subcloned into the binary vector pBI101.3 upstream of the *GUS* coding sequence (Clontech, Saint-Germain-en-Laye, France). Plant transformation, using *Agrobacterium tumefaciens* strain LBA4404, was performed by the floral dip method (Clough and Bent, 1998). Transformants were selected on 80 μg/ml kanamycin. GUS staining was carried out as described (Sessions et al., 1999), with 10 mM $K_3Fe(CN)_6$ and 10 mM $K_4Fe(CN)_6$, to limit stain diffusion. Plant samples were destained in 75% ethanol and digital images were taken with a Coolpix 995 camera (Nikon, Champigny sur Marne, France).

A 4.9 kb stretch of *KNAT1* (*BP*) promoter sequence upstream of the translation initiation site was amplified from wild-type WS *Arabidopsis* using primers 5′-GCGGCCGCTTCGGTGTGTGATTAGTGAT-3′ and 5′-ACTAGTACCCAGATGAGTAAAGATTT-3′ and cloned as a *Not*I-*Spe*I fragment upstream of the ALCR sequence in the pLP999 vector that also contains an AlcA:erGFP cassette (Deveaux et al., 2003). Plant transformation and selection were as previously described (Deveaux et al., 2003).

Immunolabelling of pectins

Immunolabelling of demethylesterified HG was conducted on transverse sections of meristems using 2F4 antibodies (Liners et al., 1989). All immunolabelling experiments were carried out using a buffer containing 0.5 mM $CaCl_2$ and milk as previously described (Peaucelle et al., 2008).

In situ hybridisation

An antisense probe of the full-length ORF of *PME5* was synthesised in vitro and labelled by DIG-UTP using a gel-purified PCR product that included the T7 RNA polymerase binding site as template. Tissue fixation, embedding, sectioning and in situ hybridisation were as described (Laufs et al., 1998), with the following changes: after dehydration of the tissues on the slide, an additional pre-hybridisation step was performed (2 hours at 45°C in 50% formamide, 5× SSC, 100 μg/ml tRNA, 50 μg/ml heparin, 0.1% Tween 20). Hybridisation was overnight at 45°C using

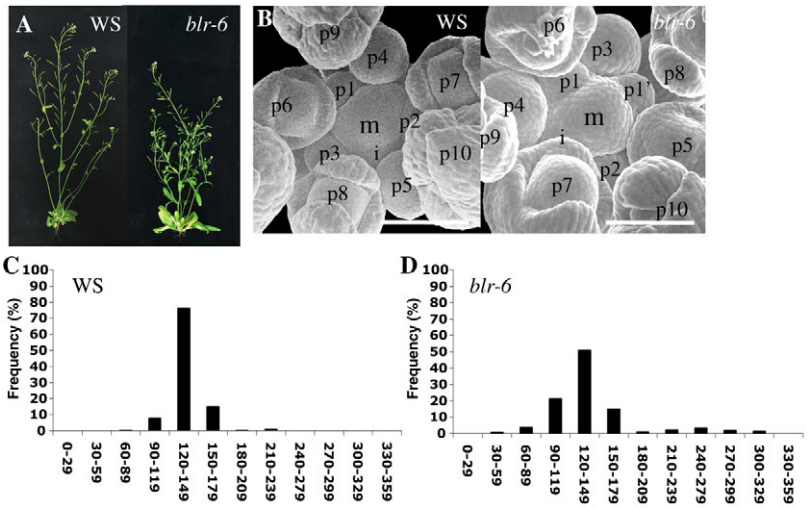

Fig. 1. Altered phyllotaxis in the meristem of the *Arabidopsis blr-6* mutant. (**A**) Overall architecture of wild type (ecotype WS) (left) and *blr-6* mutant (right) presenting abnormal phyllotaxis. (**B**) Ectopic primordia formation in *blr-6* compared with wild type as revealed by scanning electron microscopy. Meristem (m), incipient primordia (i) and growing primordia (p1-10) are indicated. Note the ectopic primordium p1′ in the *blr-6* mutant. Scale bars: 200 μm. (**C**,**D**) Meristematic phyllotaxis in wild type [total number of measurements (*n*)=298, average (av)=137.5, s.d.=16.1] and *blr-6* (*n*=333, av=142.0, s.d.=45.9). Divergence angles between two successive flowers in the meristem were allocated into twelve 30° classes and the percentage of total measurements (*n*) falling into each is displayed.

DakoCytomation mRNA In Situ Hybridisation Solution (Dako, Trappes, France). Washing was as described previously, except that a first washing step (0.1× SSC, 0.5% SDS, 30 minutes at 45°C) and a second washing step (2× SSC, 50% formamide, 60 minutes at 45°C) were included.

RESULTS

Altered phyllotaxis in the *Arabidopsis blr-6* mutant

We identified *blr-6*, a new allele of the *BLR* gene in the wild-type WS background (see Materials and methods). The *blr-6* mutant is characterised by the production of ectopic flowers at the shoot apex and by a high proportion of short internodes (Fig. 1A,B). To characterise the phyllotactic defect, we studied the pattern of organ initiation in wild-type and *blr-6* SAMs by measuring the angles between successive primordia (Fig. 1B). As shown in Fig. 1C,D, the divergence angle distribution was significantly different between *blr-6* and the wild type (P=2.8×10^{-5}, K-S test). In *blr-6*, the divergence angle showed a bimodal distribution with peaks at 120-149° and 240-279°. The distribution of the angles around 137° was similar to that of the wild type but with a higher variability (s.d.=46 versus s.d.=16 in wild type). The primordia with angles of 240-279° can be considered ectopic as they do not follow the normal phyllotactic pattern. In conclusion, the pattern of organ initiation in the *blr-6* meristem presents two defects: higher variability in the positioning of successive primordia within a normal phyllotactic pattern and ectopic primordia formation.

Increased pectin demethylesterification in the SAM of *blr-6*

To investigate whether the ectopic primordia of the *blr-6* mutant could be related to changes in cell wall composition within the SAM, Fourier transform infrared (FTIR) microspectroscopy was carried out on a 50 μm × 50 μm region delimiting the central meristem dome on a 12 μm transverse section through the shoot apex (Fig. 2A,B). We compared wild-type and *blr-6* FTIR spectra using a *t*-test for each wave number. Only two wave numbers (1720 cm^{-1} and 1780 cm^{-1}), which correspond to ester bonds, showed significant differences in absorbance (higher in wild type than in *blr-6*). Esters are mainly found in cell wall pectin. These results suggest a lower degree of HG esterification in the *blr-6* meristem in the absence of other changes in cell wall composition detectable with this sensitive technique.

To confirm the changes in pectin structure in the SAM of the *blr-6* mutant, pectic epitopes were immunolocalised on successive transverse sections of the meristem with monoclonal antibody 2F4, which specifically labels demethylesterified HG (Liners et al.,

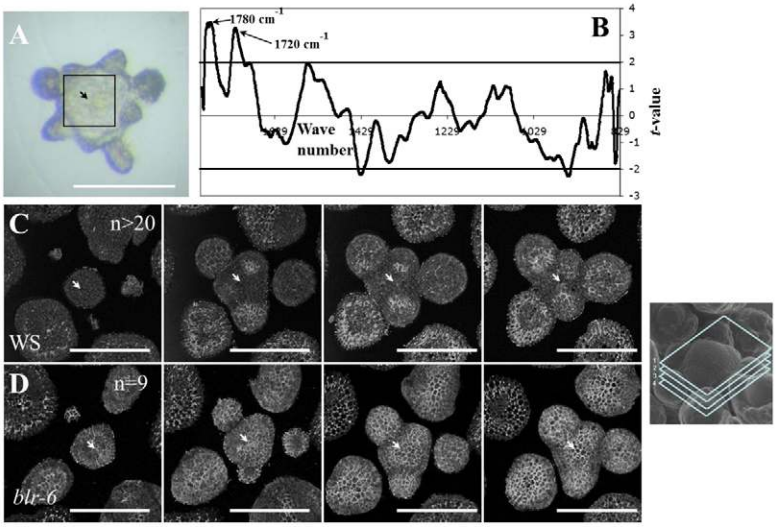

Fig. 2. Reduced pectin methylesterification in the meristem in *blr-6*. (**A**) A 12 μm meristem slice, indicating the area (square) in which the FTIR spectrum in B was acquired. (**B**) Student's *t*-test on the comparison between FTIR spectra collected from wild-type and *blr-6* meristems. Arrows indicate wave numbers for which differences are significant (P<0.01). (**C**,**D**) Immunolabelling of demethylesterified pectins using 2F4 antibody on four successive 6 μm transverse sections (starting from the meristem surface, shown on the right) of WS and *blr-6* meristems. Arrows indicate the central zone of the meristem. Scale bars: 100 μm.

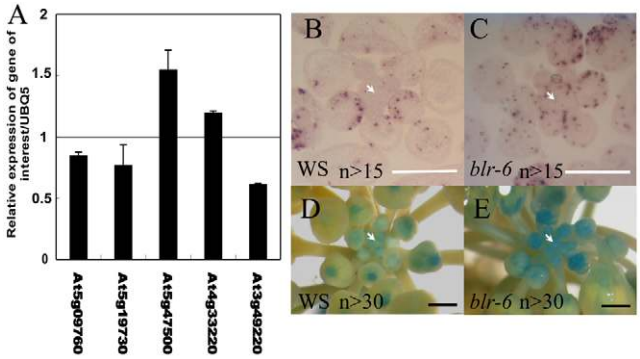

Fig. 3. *PME5* transcript levels are upregulated in *blr-6*. (**A**) Transcript levels of five putative meristem-expressed pectin methylesterase genes in floral buds of *blr-6*. Levels in wild type are set at 1. Error bars indicate s.d. (n=4-6). (**B**,**C**) In situ hybridisation of *PME5* transcripts on transverse sections of WS and *blr-6* meristem. (**D**,**E**) Binocular observations of the meristem of WS and *blr-6* *Arabidopsis* plants containing a p*PME5::GUS* construct, following GUS staining and tissue-clearing in ethanol. Arrows indicate the central zone of the meristem. Scale bars: 100 μm.

1989). As previously described, in the wild type the centre of the meristem dome remained unlabelled, while 2F4 labelling was observed in the walls of young primordia (Fig. 2C) (Peaucelle et al., 2008). By contrast, in the *blr-6* mutant the 2F4 signal was more widespread and stronger throughout the entire section (Fig. 2D). These results, together with the FTIR data, show that the degree of methylesterification of HG was greatly reduced in the mutant meristem. Such a decrease in the degree of methylesterification of *blr-6* most likely reflects higher activity of the pectin-modifying enzyme pectin methylesterase (PME).

Ectopic expression of *PME5* in *blr-6*

To investigate whether higher pectin demethylesterification in the floral buds of the *blr-6* mutant was the result of increased expression of PME genes, we first exploited microarray databases (http://bar.utoronto.ca/efp/cgi-bin/efpWeb.cgi) to identify PMEs expressed in the SAM. The expression of five meristem-expressed PMEs was further analysed by RT-qPCR (Fig. 3A). PMEs *At5g47500* and *At4g33220* were upregulated (1.6- and 1.2-fold, respectively) in the *blr-6* mutant compared with wild type. *At5g47500* (referred to as *PME5*) is the most highly expressed PME family member in wild-type inflorescence meristems (data not shown) and its overexpression in the SAM induces ectopic flower primordia formation (Peaucelle et al., 2008). *PME5* was therefore chosen for more detailed analysis.

In situ hybridisation on wild-type floral buds revealed the presence of *PME5* transcripts exclusively in young primordia in a salt and pepper pattern typical for cell cycle-regulated transcripts (Fig. 3B). In the *blr-6* mutant, however, *PME5* transcripts were observed at ectopic positions in the meristem dome in addition to the young primordia (Fig. 3C).

To investigate whether the higher *PME5* mRNA levels could be related to modified transcriptional regulation, we analysed *PME5* promoter activity in wild-type and *blr-6* mutant backgrounds using a *PME5* promoter::GUS reporter. Increased GUS staining was observed in the *blr-6* mutant, in particular in the meristem dome, compared with the wild type (Fig. 3D,E). However, in contrast to the in situ hybridisation results, the GUS staining was homogenous, suggesting that either the promoter fragment was lacking the information needed for cell cycle regulation, or that this regulation occurred at a post-transcriptional level. Nevertheless, the higher promoter activity of *PME5* in the mutant background suggests that the BLR protein negatively regulates *PME5* transcription in the wild-type meristem dome.

Reduced PME activity in floral buds and reduced variability in primordia position in *pme5* mutants

We previously showed that ectopic PME activity leads to ectopic primordia formation, whereas inhibition of PME activity blocks primordia outgrowth (Peaucelle et al., 2008). Here, we investigated whether a reduction in PME5 expression also could affect primordia positioning. We first isolated two mutants, *pme5-1* (175B12) and *pme5-2* (232E12), which carry T-DNA insertions in the first and third exon, respectively (see Fig. S1A in the supplementary material). Both mutants can be considered null as no *PME5* transcripts are detected in floral buds by RT-qPCR (see Fig. S1B in the supplementary material). The absence of *PME5* transcripts in the *pme5-1* meristem was further confirmed by in situ hybridisation (see Fig. S1C in the supplementary material). PME assays (using standard conditions, see Materials and methods) on cell wall-enriched protein extracts from flower buds showed that total PME activity was ~60% of that of the control in both *pme5-1* and *pme5-2* lines (Fig. 4A and see Fig. S1D in the supplementary material).

We next compared the phyllotaxis of wild-type and *pme5-1* meristems. Interestingly, *pme5-1* differed significantly from the wild type in the divergence angle distribution in the meristem (P=0.011, P=0.009 and P=0.0089 by K-S test in three independent experiments) and with a smaller standard deviation (*pme5*, s.d.=10.1, 7.4, 9.0; wild type, s.d.=16, 15, 19).

As a control, the statistical test failed to distinguish between the distributions of the three biological repeats for the wild-type samples (P=0.70, P=0.70 and P=0.71 for experiment 1 versus 2, 1 versus 3, and 2 versus 3, respectively) (Fig. 4B,C). The reduced PME activity in *pme5-1* therefore correlates with a reduced variability in primordia positioning in the meristem.

pme5-1 complements the ectopic primordia phenotype of *blr-6*

We next investigated the relationship between the altered phyllotaxis, the increased pectin demethylesterification and the ectopic expression of *PME5* in the *blr-6* meristem. We first assayed total PME activity in floral buds. The activity was 3-fold higher in the *blr-6* mutant than in the wild type (Fig. 4A), which could suggest post-transcriptional or post-translational control of PME activity.

Next, we generated and analysed a *blr-6/pme5-1* double mutant. In the double mutant, PME activity was greatly reduced compared with *blr-6*, indicating that the ectopic expression of *PME5* explains most of the increased PME activity in *blr-6* (Fig. 4A). Interestingly, the divergence angle distribution in the meristems of the double mutant was indistinguishable from that of *pme5-1* (P=0.3, P=0.78, P=0.45 by K-S test in three independent experiments) and significantly different from that of *blr-6* ($P<1\times10^{-4}$, $P<1\times10^{-4}$, P=0.001 by K-S test in three independent experiments) (Fig. 4C-E).

To confirm that the phyllotactic pattern observed in *blr-6/pme5-1* is due to the absence of PME5 activity, we ectopically expressed *PME5* under the control of the constitutive 35S promoter in the double mutant. Double mutants expressing *35S:PME5* indeed

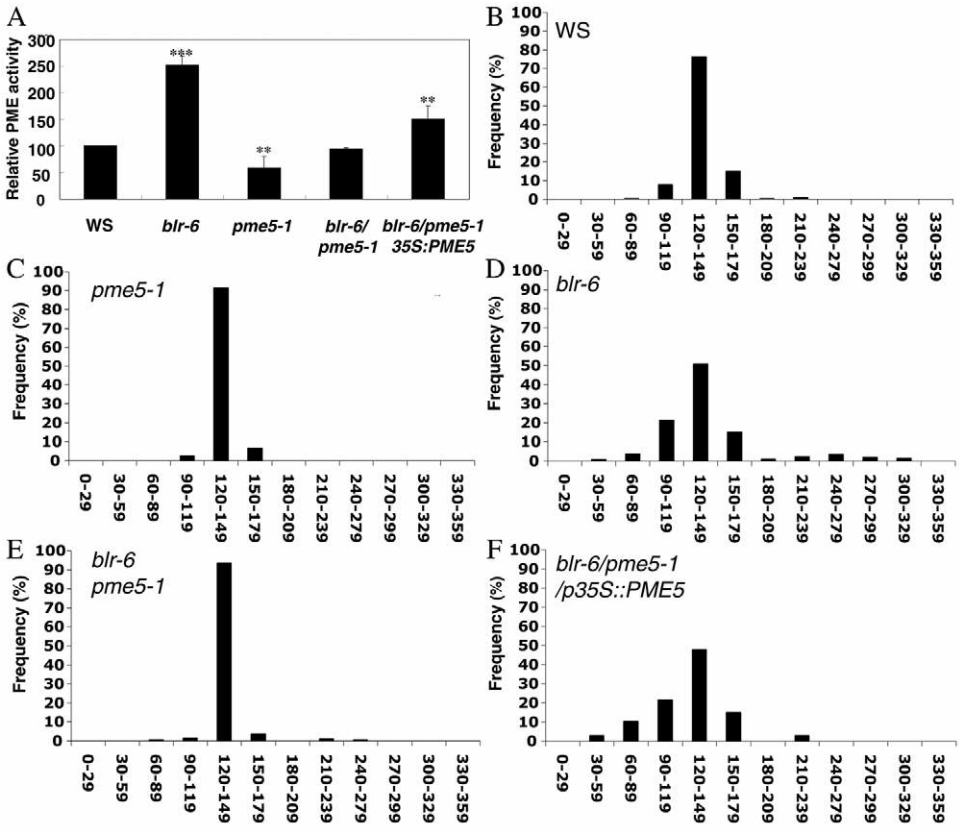

Fig. 4. PME activity levels and meristematic phyllotaxis in wild-type and mutant backgrounds. (**A**) PME activity measured on inflorescence buds of WS, *pme5-1*, *blr-6*, *blr-6/pme5-1* and *blr-6/pme5-1/p35S::PME5*. PME activity data were statistically analysed by the Mann-Whitney test. **, $P<0.01$; ***, $P<0.001$. Error bars indicate s.d. (n=4-6). (**B-F**) Meristematic phyllotaxis in wild type (n=298, av=137.5, s.d.=16.1), *pme5-1* (n=227, av=137.80, s.d.=10.1), *blr-6* (n=333, av=142.0, s.d.=45.9), *blr-6/pme5-1* (n=215, av=136.4, s.d.=8.9) and *blr-6/pme5-1/p35S::PME5* (WS background, n=107, av=12.8, s.d.=32.8). Divergence angles between two successive flowers in the meristem were allocated into twelve 30° classes and the percentage of total measurements (n) falling into each is displayed. Reduction in PME activity in the *pme5-1* mutant leads to reduced variability in the phyllotactic pattern observed in the meristem compared with the wild type. In the *blr-6/pme5-1* double mutant, the variability in phyllotaxis observed in *blr-6* is rescued. Ectopic expression of PME5 using a p*35S::PME5* construct induced increased variability in the *blr-6/pme5-1* double mutant.

showed a higher PME activity than that of *blr-6/pme5-1* (Fig. 4A) and a phyllotaxis in the meristem that was indistinguishable from that of the *blr-6* mutant (Fig. 4D,F).

Together, these results indicate that the increased PME activity and the abnormal phyllotactic pattern in the meristem in *blr-6* are solely the result of the ectopic expression of *PME5*. Strikingly, as discussed below, the disordered post-meristematic phyllotaxis phenotype observed in *blr-6* was not rescued in *blr-6/pme5-1* (see Fig. S2 in the supplementary material). We show that this can be explained by an independent role for *PME5* in the regulation of internode length.

Expression of *PME5* is downregulated in the internodes of *blr-6*

To investigate the potential role of *PME5* in regulating internode length and the post-meristematic maintenance of phyllotaxis, we first analysed the activity of the *PME5* promoter in wild-type and *blr-6* mutant backgrounds using *PME5* promoter::GUS transformants. The *PME5* promoter was active in wild-type but not in *blr-6* internodes (Fig. 5). This suggests that, in the internode, BLR acts as an activator of *PME5* transcription, in contrast to the meristem, where BLR appears to act as a repressor. In the context of the *blr-6* mutant, the post-meristematic phyllotaxis phenotype (i.e. short internodes) might thus be related to the lack of *PME5* expression in the internode.

pme5-1 does not complement the post-meristematic phyllotaxis phenotype of *blr-6*

To analyse the post-meristematic modifications of phyllotaxis, we first compared the internode length of *blr-6*, *pme5-1* and *blr-6/pme5-1* mutants with that of the wild type. No significant differences were detected between wild-type and *pme5-1* plants for this parameter (Fig. 6A; P=0.139, P=0.131, P=0.611 by K-S test in three independent experiments). By contrast, *blr-6* and *blr-6/pme5-1* plants presented a phenotype of large variability in internode length and, notably, a high frequency of shorter internodes (Fig. 6B,C; $P<0.001$ by K-S test in three independent experiments). Similar results were obtained for the variability in the divergence angles of the siliques along the stem (see Fig. S3A-C in the supplementary material).

The observed decrease in internode length (Fig. 6B,C) was related to a decreased length of epidermal cells, as shown in *blr-6* and *blr-6/pme5-1* mutants. For example, the average cell length in the *blr-6* mutant was about one-sixth that of the wild type (5.3±5.1 μm versus 32±14 μm), whereas no such differences were observed for the *pme5-1* single mutant compared with the wild type (Fig. 7A-C).

Expression of *PME5* in the internodes of *blr-6* partially rescues the post-meristematic maintenance of phyllotaxis

Next, we investigated whether *PME5* expression in the internode could restore post-meristematic maintenance and cell elongation in the *blr-6* mutant. We used the promoter of *KNAT1*, which shows the same expression pattern as *PME5* in the internodes (Fig. 5A,C). Internode length and cell length within short internodes were measured in *blr-6* expressing *PME5* under the control of the *KNAT1* promoter. The expression of *PME5* in *blr-6* internodes rescued the post-meristematic phenotype, as shown by the increase in internode length compared with *blr-6* (Fig. 6D) and the rescue of the defects in post-meristematic phyllotaxis (see Fig. S3D in the supplementary material). The observed increase in internode length was related to an increased cell length (Fig. 7D; P=0.11, P=0.19,

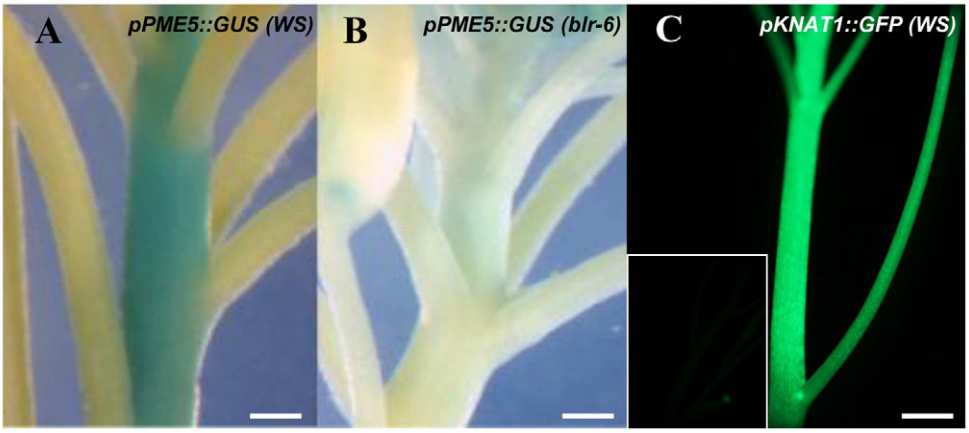

Fig. 5. *PME5* and *KNAT1* promoter activity in the stem. (**A**,**B**) *PME5* promoter activity in the stem of WS (A) and *blr-6* (B) *Arabidopsis* plants. Binocular observations of inflorescences of WS and *blr-6* plants containing a p*PME5::GUS* construct, following GUS staining and tissue-clearing in ethanol. (**C**) *KNAT1* promoter activity in WS plants. Binocular observation of inflorescences of WS containing a p*KNAT1*::GFPi construct following ethanol induction. The inset shows non-induced plants. Scale bars: 0.5 cm.

P=0.22, K-S test in three independent experiments). This confirms that, in *blr-6*, the post-meristematic defect in phyllotaxis is due to reduced *PME5* expression in the internodes.

To investigate whether the ectopic PME activity in the meristem could be indirectly responsible for the reduced internode elongation and altered post-meristematic phyllotaxis, we expressed *PME5* under the control of the meristem-specific *UFO*-derived promoter. Similar internode and cell lengths as well as divergence angles at the post-meristematic levels were observed in *UFO::PME5* lines and wild-type plants (see Fig. S4 in the supplementary material), confirming that internode elongation is not affected by ectopic *PME5* expression in the meristem. These results show that the altered post-meristematic phyllotaxis in *blr-6* is a result of the downregulation of *PME5* in the internode rather than of ectopic *PME5* expression in the meristem.

We conclude that, in wild-type plants, *PME5* plays a dual role in controlling phyllotaxis at the meristematic and post-meristematic level. This involves organ-specific regulation of the expression of *PME5* by BLR.

DISCUSSION

BLR was previously shown to be required for the maintenance of meristem identity in the SAM. BLR transcripts are present in the meristem and are downregulated in incipient primordia (Byrne et al., 2003). In loss-of-function *blr* mutants, such as *blr-6* used in this study, phyllotaxis is perturbed, with an increased variability in the divergence angles and ectopic primordia (Byrne et al., 2003; Smith et al., 2003). BLR forms heterodimers with the KNOX TALE homeodomain protein STM and acts in combination with two other BEL1-like homeodomain proteins, PNF and ATH1 (Belles-Boix et

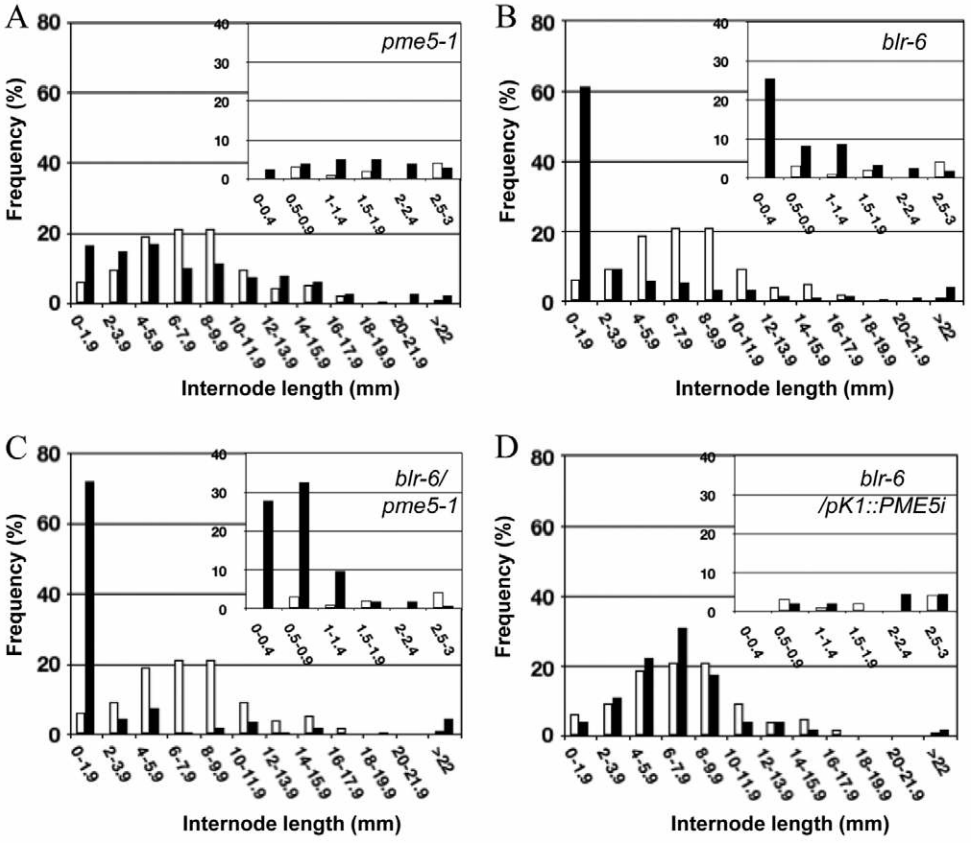

Fig. 6. Internode length in *pme5-1*, *blr-6*, *blr-6/pme5-1* and *blr-6/pKNAT1:PME5i Arabidopsis* plants. (**A-D**) Distribution of internode length between two successive flowers along the stem. The percentage of total internode lengths falling into each of twelve classes of 2 mm are shown. Insets show a finer distribution of internodes shorter than 3 mm, in classes of 0.5 mm. White bars represent data obtained for wild type (*n*=285, av=147, s.d.=49 and av=9.4 mm, s.d.=6.3 mm) and black bars for (A) *pme5-1* (*n*=300, av=147, s.d.=47 and av=8.5 mm, s.d.=5.8 mm), (B) *blr-6* (*n*=344, av=162, s.d.=90 and av=2.0 mm, s.d.=2.5 mm), (C) *blr-6/pme5-1* (*n*=162, av=178, s.d.=96 and av=3.4 mm, s.d.=6.4 mm) and (D) *blr-6/pKNAT1:PME5i* (*n*=65, av=133, s.d.=35 and av=9.2 mm, s.d.=6.9 mm). In the case of the *blr-6/pKNAT1:PME5* plants, measurements were carried out 4 weeks after a 5-day ethanol induction.

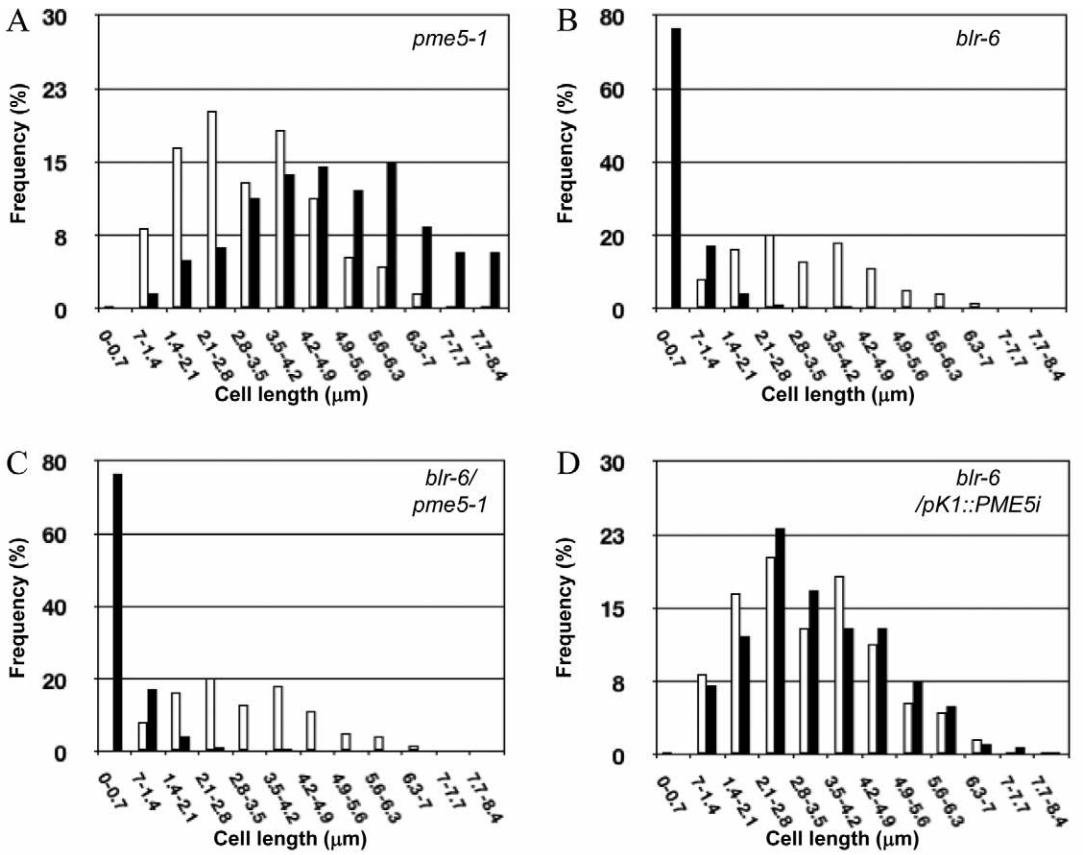

Fig. 7. Length of stem epidermal cells in *pme5-1*, *blr-6*, *blr-6/pme5-1* and *blr-6/pKNAT1:PME5i Arabidopsis* plants. (**A-D**) The percentage of cell lengths, as measured on short internodes (shorter than 1 mm), falling into each of twelve classes of 0.7 μm. White bars represent data obtained for wild type (*n*=301, av=320 μm, s.d.=143 μm) and black bars for (A) *pme5-1* (*n*=239, av=483 μm, s.d.=172 μm), (B) *blr-6* (*n*=391, av=74 μm, s.d.=102 μm), (C) *blr-6/pme5-1* (*n*=310, av=51 μm, s.d.=145 μm) and (D) *blr-6/pKNAT1*:PME5i (*n*=255, av=333 μm, s.d.=142 μm). In the case of the *blr-6/pKNAT1:PME5* plants, measurements were carried out 4 weeks after a 5-day ethanol induction.

al., 2006; Mele et al., 2003; Rutjens et al., 2009). *blr/pnf/ath1* triple mutants phenocopy the extreme *stm-1* phenotype, in which all cells in the meristem are recruited for the formation of a single primordium. By comparison, *blr-6* represents a mild phenotype, in which the ability to maintain meristem identity is only partially affected.

Here, we provided insight into the mechanism underlying the allocation of meristem cells to the developing primordium. We provide evidence that BLR represses, directly or indirectly, the expression of *PME5* in the meristem. In the *blr-6* mutant, the altered phyllotaxis in the meristem can be explained entirely by the ectopic *PME5* expression in the meristem dome, as shown by the complete restoration of meristem phyllotaxis in a *blr-6/pme5-1* double mutant. These observations support a scenario in which the demethylesterification of HG in the cell wall is a critical step in the loss of meristem identity and in the allocation of the cell to a primordium. The maintenance of meristem identity during cell division requires the inhibition of PME activity, at least partly through inhibition of the accumulation of the *PME5* transcript by BLR. This is consistent with the observation that *PMEI3* overexpression completely prevents primordia formation (Peaucelle et al., 2008). At the meristem periphery, the observed downregulation of *BLR* expression (Byrne et al., 2003) is likely to cause *PME5* transcript accumulation. Demethylesterification of HG in the newly deposited cell wall is sufficient for the recruitment of the cell into the primordium, as shown by the formation of ectopic primordia upon ectopic *PME5* expression. In this scenario, it is interesting to note that the primordium fate is determined negatively by the loss of meristem identity, as a result of derepression of *PME5*. Primordia patterning is based on the positive determination of cells in the initium by local accumulation of the phytohormone auxin (Bayer et al., 2009; Reinhardt et al., 2000; Reinhardt et al., 2003; Yu et al., 2009). This might impinge on *PME5* expression directly or indirectly, possibly via BLR.

It should also be noted that *pme5-1* rescues the altered phyllotactic pattern in the *blr-6* meristem but not the altered distribution of flowers and siliques in the mature inflorescence. This defect reflects changes in the post-meristematic elongation of the internodes, as revealed by the decreased length of internode epidermal cells in *blr-6*. Since the promoter activity of *PME5* was repressed in the internode of *blr-6* mutants, this suggests that, depending on the tissue, BLR can either act as an inhibitor or activator of *PME5* expression (Fig. 8). This hypothesis is in accordance with the reported expression of *BLR* in stems (Byrne et al., 2003). The constitutive, or inducible, expression of *PME5* in the internodes complemented the *blr-6* phenotype, which confirms the role of the pectin methylesterification status in the control of internode cell elongation. Such a role of PME-mediated changes in cell elongation is in accordance with previous data obtained on hypocotyls (Pelletier et al., 2010). However, the absence of a post-meristematic phenotype in the *pme5-1* single mutant could be related to potential redundancy within the large PME gene family.

How does demethylesterification of HG lead to primordia formation? This chemical change is expected to cause dramatic changes in the physicochemical properties of the polymer, but also removes the protection against hydrolysis by the pectin-hydrolysing enzymes pectate lyase and polygalacturonase. Cleavage of HG reduces its viscosity and presumably leads to an increase in the porosity of the cell wall, which in turn may facilitate the access of other cell wall-loosening agents, such as expansins, to their substrates (Fleming et al., 1997; Reinhardt et al., 1998). We recently investigated the role of PME5-mediated HG demethylesterification

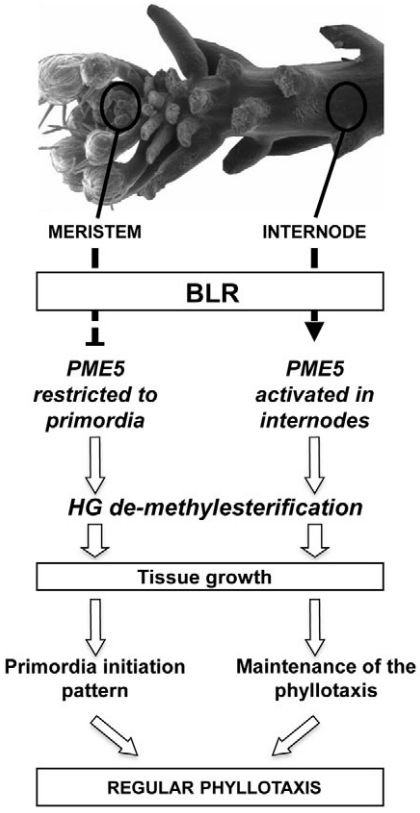

Fig. 8. The opposing effects of BLR on the expression of *PME5* in the wild-type meristem and internode and the impact on the establishment and maintenance of the phyllotactic pattern. BLR acts, directly or indirectly, to regulate *PME5* transcription in a tissue-specific manner. BLR represses *PME5* expression in the meristem, leading to demethylesterification of pectins that is restricted to primordia, thus influencing the establishment of the phyllotactic pattern. By contrast, BLR activates *PME5* expression in the internode, promoting cell elongation and the post-meristematic maintenance of phyllotaxis. The tissue-specific regulation of *PME5* expression by BLR thus directs regular phyllotaxis patterning.

in the mechanical properties of the meristem. Using micro-indentation we demonstrated that HG demethylesterification does not lead to the predicted stiffening of the pectic matrix but rather to a local reduction of cell wall rigidity (Peaucelle et al., 2011). This is likely to be related to the mode of action of PME isoforms (blockwise versus non-blockwise) that could generate substrates for pectin-degrading enzymes. Our data, together with data presented in previous work (Peaucelle et al., 2008), suggest that BLR-controlled HG demethylesterification could be one of the key elements controlling the mechanical changes that underlie organ formation. In this respect, it is likely that changes in pectin structure could act synergistically with the regulation of the microtubule cytoskeleton and changes in PIN polarity, affecting auxin transport through mechanical stresses and thus triggering morphogenesis at the shoot apex (Hamant et al., 2008; Heisler et al., 2010). Our results could pave the way to adding novel components to the current model for phyllotaxis through integrating PIN1, the regulation of cell wall structure and cell mechanics.

Funding
This work was supported by the Agence Nationale de la Recherche [grants ANR-09-BLANC-0007-01 GROWPEC and ANR-10-BLAN-1516 MECHASTEM].

Competing interests statement
The authors declare no competing financial interests.

Supplementary material
Supplementary material for this article is available at
http://dev.biologists.org/lookup/suppl/doi:10.1242/dev.072496/-/DC1

References
Bainbridge, K., Guyomarc'h, S., Bayer, E., Swarup, R., Bennett, M., Mandel, T. and Kuhlemeier, C. (2008). Auxin influx carriers stabilize phyllotactic patterning. *Genes Dev.* **22**, 810-823.
Bao, X., Franks, R. G., Levin, J. Z. and Liu, Z. (2004). Repression of AGAMOUS by BELLRINGER in floral and inflorescence meristems. *Plant Cell* **16**, 1478-1489.
Bayer, E. M., Smith, R. S., Mandel, T., Nakayama, N., Sauer, M., Prusinkiewicz, P. and Kuhlemeier, C. (2009). Integration of transport-based models for phyllotaxis and midvein formation. *Genes Dev.* **23**, 373-384.
Belles-Boix, E., Hamant, O., Witiak, S. M., Morin, H., Traas, J. and Pautot, V. (2006). KNAT6: an Arabidopsis homeobox gene involved in meristem activity and organ separation. *Plant Cell* **18**, 1900-1907.
Bradford, M. M. (1976). A rapid and sensitive method for the quantitation of microgram quantities of protein utilizing the principle of protein-dye binding. *Anal. Biochem.* **72**, 248-254.
Byrne, M. E., Groover, A. T., Fontana, J. R. and Martienssen, R. A. (2003). Phyllotactic pattern and stem cell fate are determined by the Arabidopsis homeobox gene BELLRINGER. *Development* **130**, 3941-3950.
Caffall, K. H. and Mohnen, D. (2009). The structure, function, and biosynthesis of plant cell wall pectic polysaccharides. *Carbohydr. Res.* **344**, 1879-1900.
Carraro, N., Peaucelle, A., Laufs, P. and Traas, J. (2006). Cell differentiation and organ initiation at the shoot apical meristem. *Plant Mol. Biol.* **60**, 811-826.
Clough, S. J. and Bent, A. F. (1998). Floral dip: a simplified method for Agrobacterium-mediated transformation of Arabidopsis thaliana. *Plant J.* **16**, 735-743.
Deveaux, Y., Peaucelle, A., Roberts, G. R., Coen, E., Simon, R., Mizukami, Y., Traas, J., Murray, J. A., Doonan, J. H. and Laufs, P. (2003). The ethanol switch: a tool for tissue-specific gene induction during plant development. *Plant J.* **36**, 918-930.
Fleming, A., McQueen-Mason, S., Mandel, T. and Kuhlemeier, C. (1997). Induction of leaf primordia by the cell wall protein expansin. *Science* **276**, 1415-1418.
Hamant, O., Heisler, M. G., Jonsson, H., Krupinski, P., Uyttewaal, M., Bokov, P., Corson, F., Sahlin, P., Boudaoud, A., Meyerowitz, E. M. et al. (2008). Developmental patterning by mechanical signals in Arabidopsis. *Science* **322**, 1650-1655.
Heisler, M. G., Hamant, O., Krupinski, P., Uyttewaal, M., Ohno, C., Jönsson, H., Traas, J. and Meyerowitz, E. M. (2010). Alignment between PIN1 polarity and microtubule orientation in the shoot apical meristem reveals a tight coupling between morphogenesis and auxin transport. *PLoS Biol.* **8**, e1000516.
Jonsson, H., Heisler, M. G., Shapiro, B. E., Meyerowitz, E. M. and Mjolsness, E. (2006). An auxin-driven polarized transport model for phyllotaxis. *Proc. Natl. Acad. Sci. USA* **103**, 1633-1638.
Kanrar, S., Onguka, O. and Smith, H. M. (2006). Arabidopsis inflorescence architecture requires the activities of KNOX-BELL homeodomain heterodimers. *Planta* **224**, 1163-7113.
Kanrar, S., Bhattacharya, M., Arthur, B., Courtier, J. and Smith, H. M. (2008). Regulatory networks that function to specify flower meristems require the function of homeobox genes PENNYWISE and POUND-FOOLISH in Arabidopsis. *Plant J.* **54**, 924-937.
Klavons, J. A. and Bennett, A. D. (1986). Determination of methanol using alcohol oxidase and its application to methyl ester content of pectins. *J. Agric. Food Chem.* **34**, 597-599.
Laufs, P., Grandjean, O., Jonak, C., Kieu, K. and Traas, J. (1998). Cellular parameters of the shoot apical meristem in Arabidopsis. *Plant Cell* **10**, 1375-1390.
Lerouxel, O., Cavalier, D. M., Liepman, A. H. and Keegstra, K. (2006). Biosynthesis of plant cell wall polysaccharides-a complex process. *Curr. Opin. Plant Biol.* **9**, 621-630.
Liners, F., Letesson, J. J., Didembourg, C. and Van Cutsem, P. (1989). Monoclonal antibodies against pectin: recognition of a conformation induced by calcium. *Plant Physiol.* **91**, 1419-1424.
Mele, G., Ori, N., Sato, Y. and Hake, S. (2003). The knotted1-like homeobox gene BREVIPEDICELLUS regulates cell differentiation by modulating metabolic pathways. *Genes Dev.* **17**, 2088-2093.
Mohnen, D. (2008). Pectin structure and biosynthesis. *Curr. Opin. Plant Biol.* **11**, 266-277.
Mouille, G., Robin, S., Lecomte, M., Pagant, S. and Hofte, H. (2003). Classification and identification of Arabidopsis cell wall mutants using Fourier-Transform InfraRed (FT-IR) microspectroscopy. *Plant J.* **35**, 393-404.

Peaucelle, A., Morin, H., Traas, J. and Laufs, P. (2007). Plants expressing a miR164-resistant CUC2 gene reveal the importance of post-meristematic maintenance of phyllotaxy in Arabidopsis. *Development* **134**, 1045-1050.
Peaucelle, A., Louvet, R., Johansen, J. N., Hofte, H., Laufs, P., Pelloux, J. and Mouille, G. (2008). Arabidopsis phyllotaxis is controlled by the methyl-esterification status of cell-wall pectins. *Curr. Biol.* **18**, 1943-1948.
Peaucelle, A., Braybrook, S.A., Le Guillou, L., Bron, E., Kuhlemeier, C. and Hofte, H. (2011). Atomic force microscopy on living Arabidopsis shoot apical meristems reveals that pectin modification triggers cell wall softening in subepidermal tissues prior to organ initiation. *Curr. Biol.* (in press).
Pelletier, S., Van Orden, J., Wolf, S., Vissenberg, K., Delacourt, J., Ndong, Y. A., Pelloux, J., Bischoff, V., Urbain, A., Mouille, G. et al. (2010). A role for pectin de-methylesterification in a developmentally regulated growth acceleration in dark-grown Arabidopsis hypocotyls. *New Phytol.* **188**, 726-739.
Pelloux, J., Rusterucci, C. and Mellerowicz, E. J. (2007). New insights into pectin methylesterase structure and function. *Trends Plant Sci.* **12**, 267-277.
Ragni, L., Belles-Boix, E., Gunl, M. and Pautot, V. (2008). Interaction of KNAT6 and KNAT2 with BREVIPEDICELLUS and PENNYWISE in Arabidopsis inflorescences. *Plant Cell* **20**, 888-900.
Reinhardt, D., Wittwer, F., Mandel, T. and Kuhlemeier, C. (1998). Localized upregulation of a new expansin gene predicts the site of leaf formation in the tomato meristem. *Plant Cell* **10**, 1427-1437.
Reinhardt, D., Mandel, T. and Kuhlemeier, C. (2000). Auxin regulates the initiation and radial position of plant lateral organs. *Plant Cell* **12**, 507-518.
Reinhardt, D., Pesce, E. R., Stieger, P., Mandel, T., Baltensperger, K., Bennett, M., Traas, J., Friml, J. and Kuhlemeier, C. (2003). Regulation of phyllotaxis by polar auxin transport. *Nature* **426**, 255-260.
Roeder, A. H., Ferrandiz, C. and Yanofsky, M. F. (2003). The role of the REPLUMLESS homeodomain protein in patterning the Arabidopsis fruit. *Curr. Biol.* **13**, 1630-1635.
Rutjens, B., Bao, D., van Eck-Stouten, E., Brand, M., Smeekens, S. and Proveniers, M. (2009). Shoot apical meristem function in Arabidopsis requires the combined activities of three BEL1-like homeodomain proteins. *Plant J.* **58**, 641-654.
Sessions, A., Weigel, D. and Yanofsky, M. F. (1999). The Arabidopsis thaliana MERISTEM LAYER 1 promoter specifies epidermal expression in meristems and young primordia. *Plant J.* **20**, 259-263.
Sieber, P., Wellmer, F., Gheyselinck, J., Riechmann, J. L. and Meyerowitz, E. M. (2007). Redundancy and specialization among plant microRNAs: role of the MIR164 family in developmental robustness. *Development* **134**, 1051-1060.
Smith, H. M. and Hake, S. (2003). The interaction of two homeobox genes, BREVIPEDICELLUS and PENNYWISE, regulates internode patterning in the Arabidopsis inflorescence. *Plant Cell* **15**, 1717-1727.
Smith, H. M., Campbell, B. C. and Hake, S. (2004). Competence to respond to floral inductive signals requires the homeobox genes PENNYWISE and POUND-FOOLISH. *Curr. Biol.* **14**, 812-817.
Smith, R. S., Guyomarc'h, S., Mandel, T., Reinhardt, D., Kuhlemeier, C. and Prusinkiewicz, P. (2006). A plausible model of phyllotaxis. *Proc. Natl. Acad. Sci. USA* **103**, 1301-1316.
Sterling, J. D, Quigley, H. F, Orellana, A. and Mohnen, D. (2001). The catalytic site of the pectin biosynthetic enzyme alpha-1,4-galacturonosyltransferase is located in the lumen of the Golgi. *Plant Physiol.* **127**, 360-371.
Stoma, S., Lucas, M., Chopard, J., Schaedel, M., Traas, J. and Godin, C. (2008). Flux-based transport enhancement as a plausible unifying mechanism for auxin transport in meristem development. *PLoS Comput. Biol.* **4**, e1000207.
Ung, N., Lal, S. and Smith, H. M. (2011). The role of PENNYWISE and POUND-FOOLISH in the maintenance of the shoot apical meristem in Arabidopsis. *Plant Physiol.* **156**, 605-614.
Yu, L., Patibanda,V. and Smith, H. M. (2009). A novel role of BELL1-like homeobox genes, PENNYWISE and POUND-FOOLISH, in floral patterning. *Planta* **229**, 693-707.